



23rd International Symposium on Nonlinear Acoustics

Nanjing, China
30 June - 4 July 2025

Signal Processing in Acoustics: Ultrasonic Imaging and Therapy

Acoustic characterization of focusing multi-element transducers and its use for imaging of objects in the focal region

Sergey A. Tsysar

Physics Faculty, Lomonosov Moscow State University, Moskovskij gosudarstvennyj universitet imeni M V Lomonosova Fiziceskij fakul'tet, Moscow, 119991, RUSSIAN FEDERATION; sergey@acs366.phys.msu.ru

Ekaterina Ponomarchuk, Petr Yuldashev, Oleg Sapozhnikov and Vera Khokhlova

Lomonosov Moscow State University Faculty of Physics: Moskovskij gosudarstvennyj universitet imeni M V Lomonosova Fiziceskij fakul'tet, Moscow, 119991, RUSSIAN FEDERATION; msu.ekaterina.ponomarchuk@gmail.com; petr@acs366.phys.msu.ru; oleg@acs366.phys.msu.ru; vera@acs366.phys.msu.ru

Accurate acoustic characterization of nonlinear focused fields is critical for pre-treatment planning and safe and effective treatments within HIFU (high-intensity focused ultrasound) applications. In this study, acoustic holography is used to measure the pressure field distribution at low-intensity and reconstruct a realistic boundary condition for a given transducer with subsequent calculation of nonlinear outcomes. A focused ultrasonic beam was generated by a fully populated 256-element concave piezocomposite array transducer with a center frequency of 1.2 MHz, a focal length of 150 mm, and an aperture of 200 mm. Multi-element HIFU arrays can also be used for pulse-echo imaging within their focal region and employed in treatment guidance and feedback. The study demonstrates that such focal imaging is feasible even for transducers consisting of large scale (several wavelengths) elements with individual narrow-beam pattern.

1. INTRODUCTION

A number of modern therapeutic ultrasound methods utilize strongly nonlinear focused fields generated by multi-element array transducers^{1,2}. Accurate acoustic characterization of such fields is critical for pre-treatment planning and safe and effective treatments. Direct measurements of nonlinear ultrasound fields are technically difficult due to the high pressure values, broad bandwidth, and strong spatial localization of shocks that are developed in the focal waveforms. Multi-element phased arrays that allow for electronic focus steering, various field configurations, and aberration correction make such characterization even more complicated. In this study, acoustic holography is used to measure the pressure field distribution at low intensity and reconstruct a realistic boundary condition for a given transducer. As the next step, an equivalent source model is constructed to produce the same acoustic field in the focal region as the real one but having axisymmetric distribution. The equivalent source then can be used for modeling nonlinear ultrasound propagation at higher power levels. An additional option that can be provided by multi-element transducers is pulse-echo imaging within their focal region for treatment guidance and feedback. The goal of this study is to demonstrate the feasibility of such imaging for transducers consisting of large-scale (several wavelengths) elements with individual narrow-beam patterns. The described approach was applied to characterizing a fully populated 256-element concave piezocomposite transducer (FPA – fully populated array) with a center frequency of 1.2 MHz, a focal length of 150 mm, and an aperture of 200 mm.

2. FIELD CHARACTERIZATION

A. ACOUSTIC HOLOGRAPHY

The acoustic pressure field distribution of an ultrasonic transducer can be reconstructed using the acoustic holography method based on a time-reversal principle³. One of the limitations of the method is the intensity level of the investigating field. In case of high intensities with peak acoustic pressure levels above several MPa in the scanning field with possible shock formation in the focal region, a number of technical difficulties arise. Broad bandwidth and strong spatial localization of the shocks require a very small mapping step for accurate field measurement, which drastically increases the number of scanning points and the measurement time. High pressure levels may damage the hydrophone during a long scanning procedure. Nonlinear effects are very sensitive to the medium parameters, which may vary during the measurements, and different spatial points of the synthesized aperture will no longer be coherent. Here we describe a combined method for low-intensity measurement and subsequent nonlinear modeling of such fields. In case of low-intensity linear mode of field propagation, the well-developed method of acoustic holography can be used. Here we illustrate the characterization procedure for the fully populated array depicted in Fig. 1.

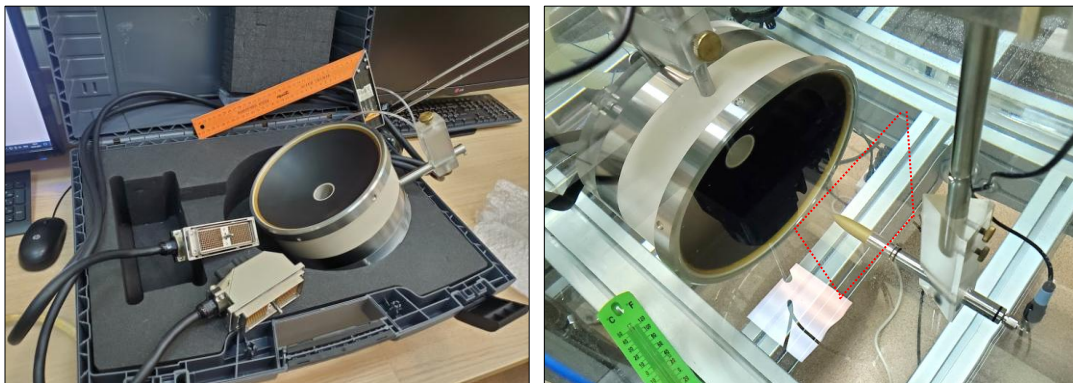


Figure 1. The fully populated array transducer consisting of 256 elements with a 200 mm aperture, a 150 mm focal distance and a 1.2 MHz central frequency (left). Typical positioning of the transducer and the scanning hydrophone during holographic measurements in a water tank (right).

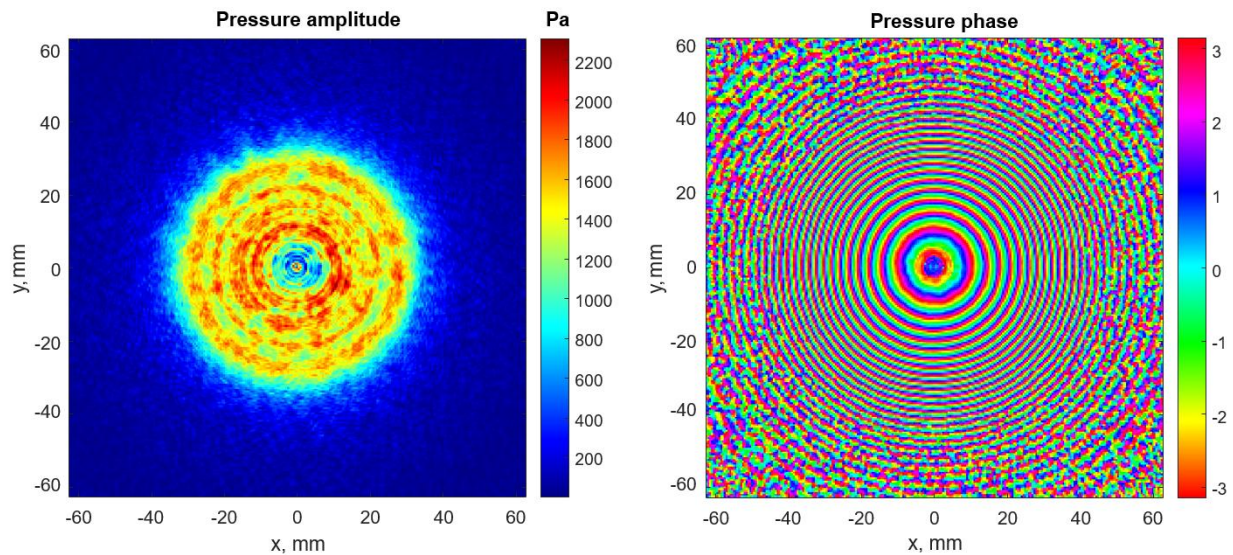


Figure 2. The acoustic pressure amplitude (left) and phase (right) for a 1.2 MHz frequency measured along the plane hologram located 100 mm from the central point of a spherical surface of the transducer.

The transducer was designed in our laboratory and manufactured by Imasonic (France) as a piezocomposite bowl divided into 256 elements in the form of densely arranged polyhedrons with a 0.5 mm kerf between the elements. The center frequency, focal length and aperture of the transducer are 1.2 MHz, 150 mm and 200 mm, respectively. It has two DL-260 Cannon connectors, each for driving 128 elements. The transducer was connected to Verasonics V-1 system using a matching network. The capsule hydrophone HGL-0200 (ONDA Corp., USA) was placed in the water tank of the UMS-3 scanning system (Precision Acoustics, UK) in front of the transducer. Water was filtered ($<10\ \mu\text{m}$) and degassed with the water treatments system (WTS, Precision Acoustics, UK) for 3 hours before the measurements. The measured acoustic pressure waveforms were averaged 16 times and captured by the TDS5054B (Tektronix, USA) digitizer for each point of a plane hologram located 50 mm prefocally. Distributions of the pressure amplitude and phase at the center operating frequency (1.2 MHz) are shown in Fig. 2.

The results of transducer surface vibration pattern reconstruction from holography data using the xDDx⁴ toolbox are presented in Fig. 3 for the 1.2 MHz normal velocity amplitude and phase.

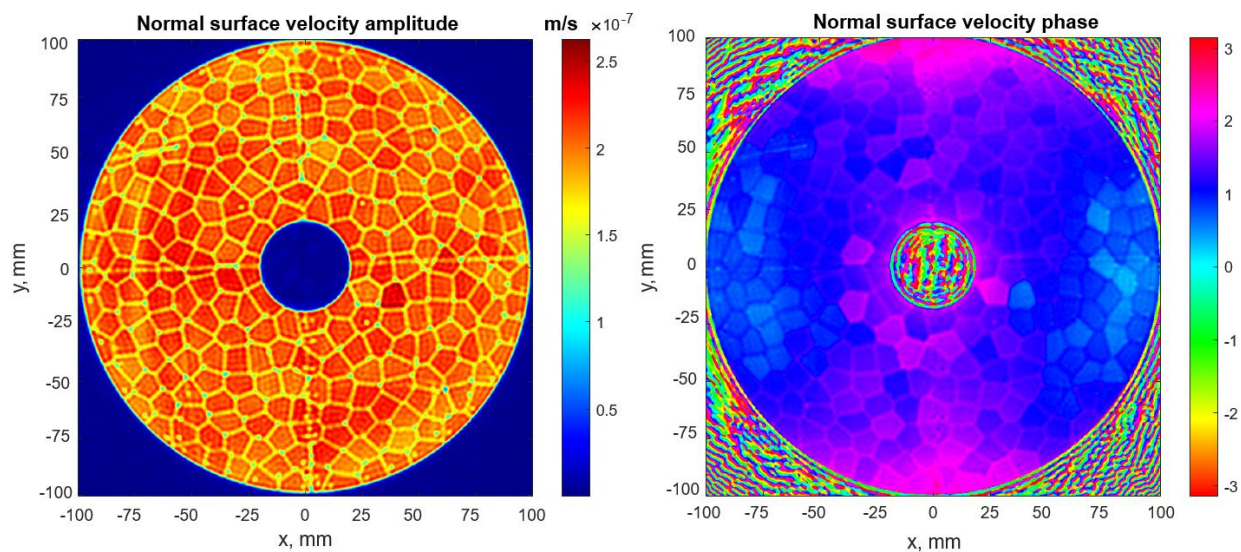


Figure 3. The acoustic pressure amplitude (left) and phase (right) for a 1.2 MHz frequency reconstructed from the measured hologram located 100 mm from the central point of a spherical surface of the transducer.

Note that the phase distribution is not uniform, which leads to the distortion of the shape of the focal region and loss of the peak pressure. Data obtained by acoustic holography can be also used to compensate for phase deviations and restore focal region parameters, as discussed in our previous paper⁵.

B. NONLINEAR FIELD CALCULATION

After the first step we obtained a realistic boundary condition for a given transducer operating in a low-intensity linear regime. As the next step, an equivalent source model was constructed to produce the same acoustic field in the focal region as the real one but with an axisymmetric distribution. The equivalent source was then used for modeling nonlinear ultrasound propagation at higher power levels using “HIFU-beam”⁶, an open-source software developed in our laboratory. The modeling allows for setting proper parameters for operating the transducer to achieve shock formation of the desired amplitude and to design the exposure protocols for sonications in strongly nonlinear regimes such as BH^{7,8} (boiling histotripsy).

3. USING THERAPEUTIC ARRAY FOR IMAGING

A. THEORY

As mentioned in the Introduction, focused multi-element therapeutic arrays can be used for imaging within a certain region around the geometrical focus. Unlike typical convex or plane imaging ultrasound probes with elements of sub-wavelength size (Fig. 4a), plane arrays consisting of larger-scale elements provide a set of narrow beams with small divergence angle $\theta \sim \lambda/D_e$ (where D_e is the typical diameter of an element), which may have no intersection in the nearfield of a transducer (Fig. 4b). At the same time, concave arrays of such elements may form an imaging region as the intersection area of individual beams for all elements (Fig. 4c). The size of this region is determined by the curvature of the array and the diameters of the individual beams near the focus. For a rough estimation of the lateral size D_F of this imaging region in focal plane of the 256-element FPA (Fig. 1) with average $D_e \approx 11$ mm we can use diffraction theory for Gaussian beams⁹ and obtain the following result.

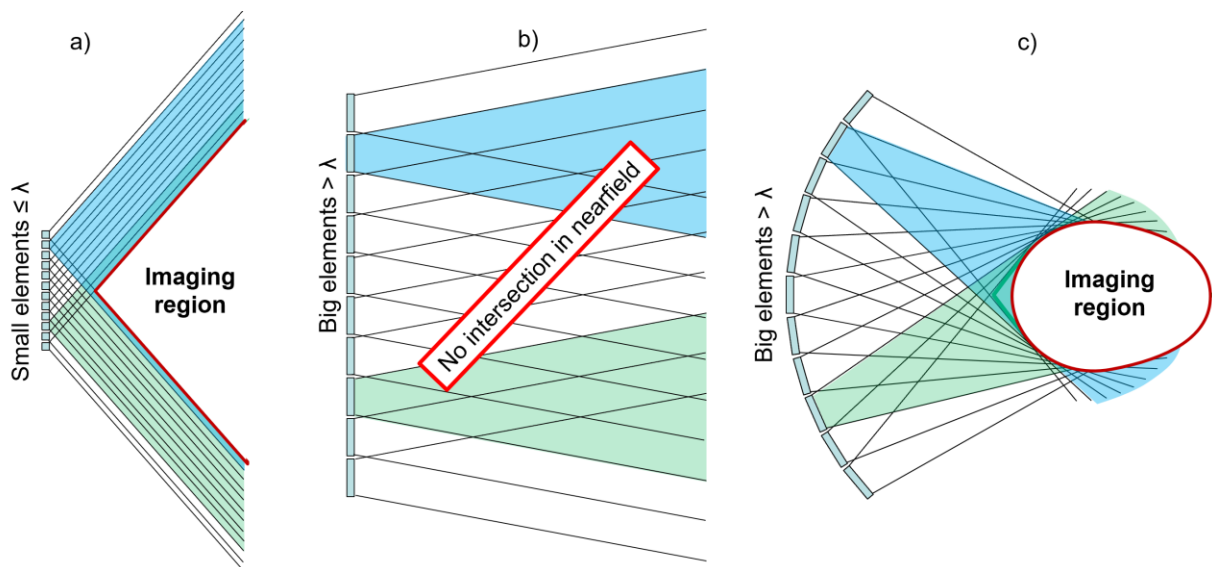


Figure 4. Schematic diagram of the imaging region formation for multi-element arrays. Individual beams of two elements are shown in color. A typical flat imaging probe with subwavelength elements (a), a flat array of larger directional elements has no imaging region in the near field (b), and a concave array of larger elements has a limited ovoid imaging region near the center of curvature of the emitting surface (c).

The diffraction length l_d for an individual beam in water with the sound speed c_0 of 1480 m/s, the central frequency f of 1.2 MHz and the following lateral size D_F in the focal region $F = 150$ mm are:

$$l_d = \frac{\pi D_e^2}{4\lambda} = \frac{\pi D_e^2 f}{4c_0} = 77.1 \text{ mm} \quad (1)$$

$$D_F = D_e \sqrt{1 + \left(\frac{F}{l_d}\right)^2} \approx 24 \text{ mm} \quad (2)$$

This value of the lateral size D_F of this imaging region in the focal plane is 8 times smaller than the aperture D_T of the transducer (200 mm), but the imaging feature in the most valuable region of interest around the geometrical focus may be useful for HIFU medical applications and for industrial applications in NDT and NDE tasks.

At the same time, the large full aperture of an array with a given focal distance provides sharp focusing with a lateral diameter d_F which determines the lateral resolution of the constructing image:

$$d_F = \frac{4F\lambda}{\pi D_T} \approx 0.95\lambda = 1.18 \text{ mm} \quad (3)$$

B. IMAGING RESULTS

The first object to image was a 1.5 mm diameter metal wire (Fig. 5a) placed in the focal plane (150 mm away from the transducer). The region available for imaging, estimated with Eq. (2), is depicted by a green dotted circle in Fig. 5. The exposure protocol was designed to generate a quasi-plane wave at the focal plane with a 1.6 V driving pulsed signal. After sonication, the echo waveforms were collected for each of the 256 channels by the Verasonics V-1 engine. Typical received signal distribution patterns for the central frequency in the form of amplitude and phase are presented in Fig. 5b and c correspondingly. Image reconstruction was performed by the conventional delay-and-sum (DAS) technique. The resulting image (Fig. 5d) confirms the estimation of the lateral size of the available region and demonstrates high resolution close to the wavelength in accordance with Eq. (3).

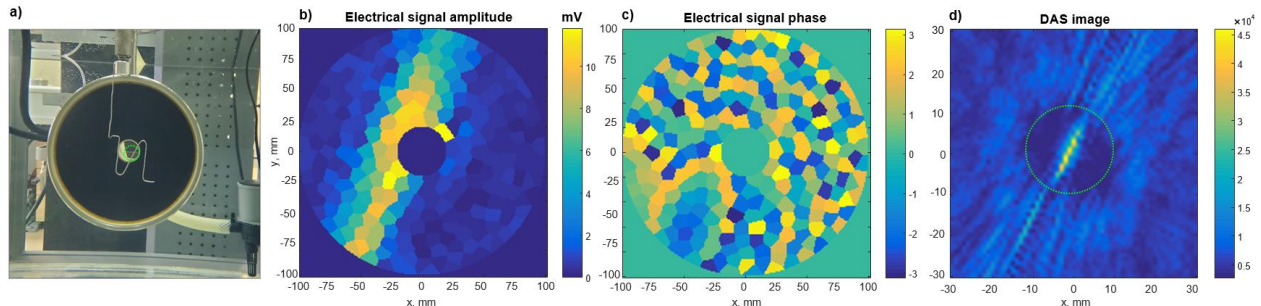


Figure 5. Imaging of a 1.5 mm wire located in the focal plane of the FPA (a). Amplitude (a) and phase (b) of the received electrical signal for each element at a 1.2 MHz frequency. The resulting image (d). The green dotted circle (a, d) represents the theoretically estimated region available for imaging by Eq. (2).

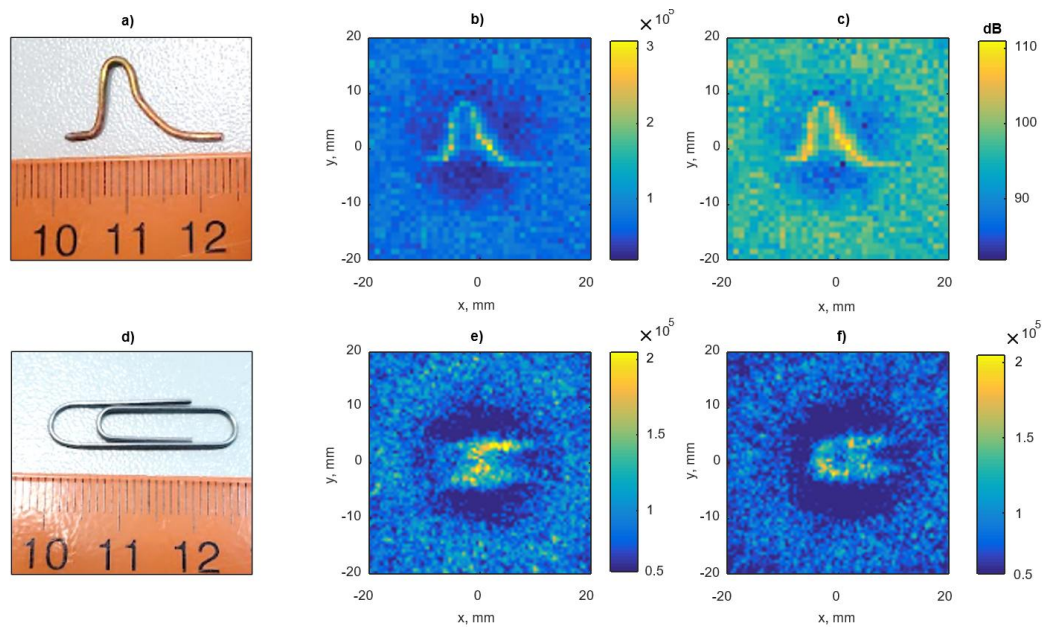


Figure 6. Imaging of a 1.2 mm (a) and a 0.8 mm (d) wire in the focal plane of the FPA. DAS reconstructed images for the 1.2 mm target in linear (b) and dB (c) scale; for the 0.8 mm target in linear scale centered (e) and 10 mm shifted along x axis (f).

Next, the targets were figures of a 1.2 mm and a 0.8 mm wire in the forms of a laboratory logo and a typical paperclip (Fig. 6a and d, correspondingly). The target of the 1.2 mm wire gave clear image within the available region: Fig. 6b represents a DAS reconstruction in linear scale, Fig. 6c – in dB scale. The SNR is about 20 dB at the lowest available excitation signal of 1.6 V. The target of the 0.8 mm wire demonstrates a 30% lower peak value and less uniform brightness on the reconstructed images (Fig. 6e and f, both in linear scale, with the target shifted 10 mm along the x axis). The main reason for this result is the sub-wavelength size of the wire.

4. CONCLUSIONS

Accurate acoustic characterization of focused transducers through acoustic holography enables precise measurement and numerical reconstruction of pressure field distributions in high-intensity focused ultrasound (HIFU) applications. This method ensures safer and more effective treatments by providing realistic boundary conditions for specific transducers. The use of multi-element transducers not only enhances precision but also allows for additional functionalities such as pulse-echo imaging and feedback, further improving treatment outcomes. The study successfully demonstrates these capabilities even for large-scale transducer elements.

ACKNOWLEDGMENTS

This work was supported by the Russian Science Foundation (grant no. 25-12-00141).

REFERENCES

- ¹ G. T. Haar, “Ultrasound focal beam surgery”. *Ultrasound. Med. Biol.* **21** (9), 1089 (1995). [https://doi.org/10.1016/0301-5629\(95\)02010-1](https://doi.org/10.1016/0301-5629(95)02010-1)
- ² G. T. Haar and C. Coussios, *Int. J. Hyperthermia*, “High intensity focused ultrasound: Physical principles and devices”. **23** (2), 89–104 (2007). <https://doi.org/10.1080/02656730601186138>

-
- ³ O. A. Sapozhnikov, S. A. Tsysar, V. A. Khokhlova, and W. Kreider, “Acoustic holography as a metrological tool for characterizing medical ultrasound sources and fields”. *J. Acoust. Soc. Am.* **138** (3), 1515–1532 (2015). <http://dx.doi.org/10.1121/1.4928396>
- ⁴ P. B. Rosnitskiy *et al.*, “xDDx: A numerical toolbox for ultrasound transducer characterization and design with acoustic holography”. *IEEE TUFFC*, **72** (5), 564–580 (2025). <http://dx.doi.org/10.1109/TUFFC.2025.3542405>
- ⁵ S. A. Tsysar *et al.*, “Phase correction of the channels of a fully populated randomized multielement therapeutic array using the acoustic holography method. *Ac. Phys.*, **70** (1), 82–89 (2024). <http://dx.doi.org/10.1134/S1063771023601280>
- ⁶ P. V. Yuldashev *et al.* “HIFU Beam: a simulator for predicting axially symmetric nonlinear acoustic fields generated by focused transducers in a layered medium”, *IEEE TUFFC*. **68** (9), 2837–2852 (2021). <https://doi.org/10.1109/tuffc.2021.3074611>
- ⁷ E. M. Ponomarchuk *et al.* “Pilot experiment on non-invasive non-thermal disintegration of human mucinous breast carcinoma ex vivo using boiling histotripsy”. *Bull. of Exp. Biol. and Med.* **177** (1), 133–136 (2024). <http://dx.doi.org/10.1007/s10517-024-06144-6>
- ⁸ E. M. Ponomarchuk *et al.* “Pilot study on boiling histotripsy treatment of human leiomyoma ex vivo”. *Ultrasound. Med. Biol.* **50** (8), 1255–1261 (2024). <http://dx.doi.org/10.1016/j.ultrasmedbio.2024.05.002>
- ⁹ M. B. Vinogradova, O. V. Rudenko, A. P. Sukhorukov. *Theory of waves*, 2nd ed. Nauka: Moscow, 1990 (in Russian)